Macromolecules **2008**, *41*, 9602−9611

Amphiphilic Linear-Hyperbranched Block Copolymers with Linear Poly(ethylene oxide) and Hyperbranched Poly(carbosilane) Block

Frederik Wurm, Hanna Schüle, and Holger Frey*

Institute of Organic Chemistry, Organic and Macromolecular Chemistry, Duesbergweg 10-14, Johannes Gutenberg-University Mainz, D-55099 Mainz, Germany

Received August 12, 2008; Revised Manuscript Received October 14, 2008

ABSTRACT: The synthesis of amphiphilic linear-hyperbranched block copolymers with a linear poly(ethylene oxide) (PEO) segment and a hyperbranched poly(carbosilane)s (PCS) block in a rapid three-step strategy is described, combining oxyanionic polymerization with carbosilane chemistry. A linear precursor block copolymer was synthesized via anionic polymerization of allyl glycidyl ether onto a commercial hydroxyl-terminated PEO, using its cesium alkoxide as macro-initiator. The resulting linear AB or ABA-type di- or triblock copolymers serve as polymer cores for the subsequent hydrosilylation polyaddition of an AB_2-type carbosilane monomer. Di(allyl)methylsilane or methyldi(undec-10-enylsilane) were employed, using Karstedt's catalyst as Pt^0-species. Due to the high reactivity of allyloxy groups in catalytic hydrosilylation reactions, the slow monomer addition technique, previously used for the controlled polyaddition of AB_2-monomers, was not necessary in this case and complete conversion of all core allyl groups is achieved. Both the molecular weights of the hyperbranched block and the linear block were varied. The resulting polymers exhibited molecular weights up to 40,100 g/mol with rather low apparent polydispersities between 1.10 and 1.47. Phase segregation of the block copolymers was investigated by differential scanning calorimetry, demonstrating strongly segregated nanophases for all block copolymers. Transition electron microscopy showed unusual anisotropic morphologies in solution, which depended both on the length of the hyperbranched block and the nature of the carbosilane monomer used.

Introduction

The synthesis of complex, branched macromolecules with well-defined polymer architecture represents an intriguing current challenge for polymer chemists. Dendritic polymers,[1] both the perfectly branched dendrimers[2] and the analogous hyperbranched materials have gathered intense interest in the past decade due to their high functionality and compact globular structure.[3] Hyperbranched polymers exhibit structural polydispersity. However, they are obtained rapidly from AB_n-type monomers, where A and B represent two mutually reactive functional groups and n determines the number of branches per repeat unit.[4] Silicon chemistry offers several quantitative reactions for the synthesis of hyperbranched or dendritic systems (i.e., hydrosilylation, Grignard reactions, and controlled condensation of silanols) that are suitable for the preparation of both highly flexible dendrimers and hyperbranched organic−inorganic hybrid materials. Among these silicon-containing dendritic polymers,[5] hyperbranched polycarbosilanes (PCS),[6] polyalkoxysilanes,[7] polycarbosiloxanes,[8] and polysiloxanes[9] have been prepared conveniently from AB_2 and AB_3 monomers.

Amphiphilic block copolymers containing a compact, dendritic block are interesting with respect to both chemical and physical behavior resulting from the constraints imposed upon the branched block by the topology. The synthesis of amphiphilic block copolymers with perfectly branched dendrimer blocks has been described,[10] based on demanding multistep approaches. However, to date only a few papers have detailed the preparation of linear-hyperbranched block copolymers that can be obtained in few synthetic steps and therefore larger quantities.[11] Such materials can exhibit unusual properties similar to those investigated for the respective linear-dendrimer hybrid block copolymers. A very recent work of Pan and coworkers describes an elegant pathway to linear-hyperbranched ABA-triblock structures based on controlled radical polymerization.[12]

Poly(ethylene oxide) (PEO) is often used as the water-soluble block for amphiphilic block copolymers. For instance, a well-understood linear amphiphilic block copolymer system is PEO-*b*-poly(butadiene) (PB).[13] Only one approach to a maximum branched hydrophobic block has been reported so far: Kim and co-workers described the synthesis of linear-dendrimer-type

Scheme 1. Structures of Linear-Hyperbranched ABA- and AB-Type Block Copolymers Based on Poly(ethylene oxide) as the Linear Segment and Branched Poly(carbosilane)s (Here Shown with Methyldiallylsilane as the Respective Monomer)

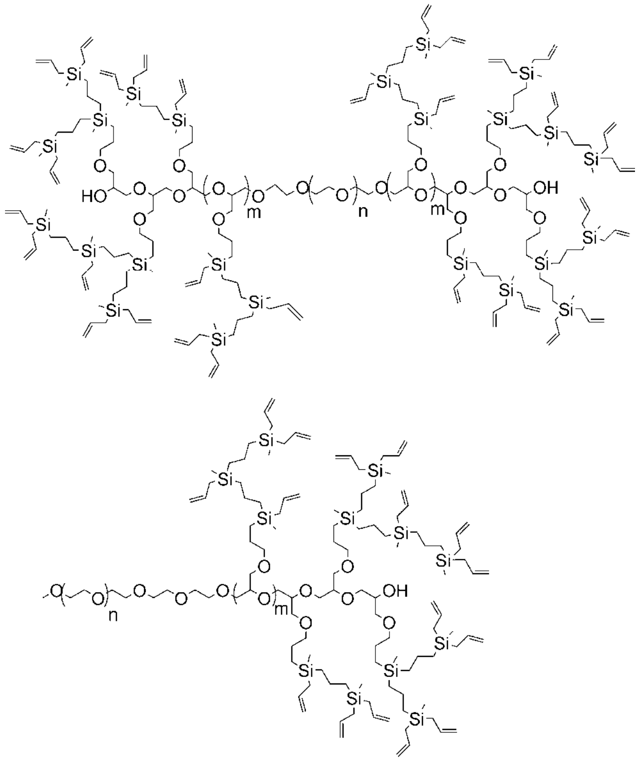

---

* Corresponding author. E-mail: hfrey@uni-mainz.de.

10.1021/ma8018427 CCC: $40.75

block copolymers, combining a linear PEO segment and a perfectly branched polycarbosilane dendrimer up to the third generation, employing a demanding multistep protocol.[14]

Here we report the first synthesis of narrow polydispersity linear-hyperbranched hybrid diblock and triblock copolymers with a water-soluble linear segment (PEO) and a hydrophobic hyperbranched block with hyperbranched polycarbosilane structure (Scheme 1). The synthesis is based on a straightforward two-step procedure, combining anionic epoxide polymerization with hydrosilylation polyaddition for the hyperbranched block.

Experimental Section

Nomenclature. Poly(ethylene oxide)-*block*-poly(allyl glycidyl ether) diblock copolymers are designated PEO$_x$-*b*-PAGE$_y$ (triblock copolymers in an analogous fashion). Hyperbranched-linear diblock copolymers are denoted by PEO$_x$-*b*-[PAGE$_n$-*hb*-MD*x*S$_m$], in which *m* indicates the degree of polymerization (DP$_n$) of the polycarbosilane block (MD*x*S). The hyperbranched block formed after grafting of the carbosilane monomers is designated [PAGE$_n$-*hb*-MD*x*S$_m$], since the PAGE block is regarded as part of the final PCS block; x represents the allyl (x = A) or the undecenyl (x = U) monomer.

Instrumentation. ^{1}H, ^{13}C, and ^{29}Si nuclear magnetic resonance spectra were recorded using a Bruker AC 300 or a Bruker AMX 400 spectrometer operated at 400 MHz for ^{1}H, employing deuterated chloroform as a solvent. ^{13}C NMR spectra (referenced internally to solvent signals) at 100.15 MHz and ^{29}Si NMR spectra (referenced externally to TMS) at 79.49 MHz.

FT-IR spectra were recorded on a Nicolet SDXC FT-IR spectrometer equipped with an ATR unit.

Size exclusion chromatography (SEC) was performed with an instrument consisting of a Waters 717 plus autosampler, a TSP Spectra Series P 100 pump and a set of three PSS-SDV 5A columns with 100, 1 000, and 10 000 Å porosity. Tetrahydrofuran was used as an eluent at 30 °C and at a flow rate of 1 mL min^{-1}. UV absorptions were detected by a SpectraSYSTEM UV2000. The specific refractive index increment (d*n*/d*c*) was measured at 30 °C on an Optilab DSP interferometric refractometer (also RI detector) and determined with the Wyatt ASTRA IV software (Version 4.90.08). Calibration was carried out using poly(styrene) standards provided by Polymer Standards Service and performing a third order polynomial fit.

Online-SEC static light scattering measurements were performed via a multiangle laser light scattering detector (MALLS) DAWN EOS laser photometer (Wyatt Technology Co.) equipped with a GaAs laser emitting at a wavelength of 685 nm. Molar masses were calculated during SEC measurements, using the Wyatt ASTRA IV software (Version 4.90.08) and ASTRA V (Version 5.1.9.1). Masses were calculated in 0.25 s intervals using the Zimm equation:

$$\frac{Kc}{R_\theta} = \frac{1}{M_w} + 2A_2c \quad \text{with } K = \frac{4\pi^2 n_0^{\,2}\left(\frac{dn}{dc}\right)^2}{\lambda_0^{\,4} N_A} \tag{1}$$

n_0 is the refractive index of toluene, N_A is Avogadro's constant, λ is the laser wavelength; M_w is the apparent weight average molecular weight, A_2 is the second virial coefficient, and R_Θ is the Rayleigh ratio of the polymer solution at a given angle. In SEC-MALLS the second virial coefficient is small enough to be neglected at the low concentrations used in chromatographic separation. As the value is unknown, we arbitrarily set it to zero, as the resulting error is very small for the low concentrations in SEC experiments.

Differential scanning calorimetry measurements were carried out on a Perkin-Elmer 7 Series Thermal Analysis System with autosampler in the temperature range of −180 to 100 °C at heating rates 10 K/min. The melting points of indium (T_0 = 156.6 °C) and Millipore water (T_0 = 0 °C) were used for calibration.

TGA measurements were conducted on a Perkin-Elmer Pyris 6 TGA.

Reagents. Poly(ethylene oxide) and poly(ethylene oxide) monomethyl ether samples were purchased from Fluka and used as received (M_n 750 g/mol, PDI 1.10; M_n 5000 g/mol, PDI 1.05; or M_n 6000 g/mol, PDI 1.06, respectively). Cesium hydroxide monohydrate (99%) and magnesium (98%) was purchased from Acros and used as received. Allyl glycidyl ether (99%) was purchased form Acros and freshly distilled from CaH$_2$ before use. Allyl bromide (97%), bromoundecene (95%), dichloromethylsilane (99%) and all solvents were purchased from Aldrich and distilled from CaH$_2$ before use. Karstedt's catalyst in xylene (2.1−2.4% Pt) was purchased from ABCR GmbH & Co. KG and used as received. Deuterated chloroform-d_1 and DMSO-d_6 were purchased from Deutero GmbH and dried and stored over molecular sieves. Methanol, chloroform, and other solvents and reagents were purchased from Acros and used as received, if not mentioned otherwise.

Synthetic Procedures. *Diallylmethylsilane (MDAS).* The monomer was synthesized according to literature procedures using[15] 68.96 g (0.57 mol) of allylbromide, 69.28 g (2.85 mol) of magnesium and 21.86 g (0.19 mol) of dichloromethylsilane. Yield: 13.82 g (57%) of a colorless liquid. Bp: 123 °C. ^{1}H NMR (300 MHz, CDCl$_3$), δ [ppm]: 5.78 (m, 2H, $-$CH=CH$_2$); 4.95−4.83 (m, 4H, $-$CH=CH$_2$); 3.79 (m, 1H, Si−H); 1.68−1.52 (m, 4H, $-$CH$_2-$CH=CH$_2$); 0.09 (d, J = 3.67 Hz, 3H, Si−CH$_3$). ^{29}Si NMR (80 MHz, CDCl$_3$), δ [ppm]: −13.98 ppm; IR (characteristic absorption bands): Q (cm^{-1}) 2115 (stretching Si−H mode), 1632 (stretching C=C mode), 1252 (stretching Si−CH$_3$ mode); 838 (stretching CH$_3$−Si−CH$_3$ mode).

Methyldiundec-10-enylsilane (MDUS). The monomer was synthesized according to literature procedures[15] using 50 g (21.4 mmol) of 11-bromoundec-1-en, 26.1 g (1.1 mol) magnesium and 8.21 g (7.1 mmol) of dichloromethylsilane. Yield: 17.4 g (75.8%) of a colorless, viscous liquid. Bp: 141 °C at 0.1 mbar. ^{1}H NMR (300 MHz, CDCl$_3$): δ (ppm) 0.05 (d, J = 3.7 Hz, 3 H, Si−CH$_3$), 0.59 (m, 4H, Si−CH$_2$), 1.2−1.5 (m, 28 H, −CH$_2$−), 2.05 (m, 4H, −CH$_2$−CH=CH$_2$), 3.77 (m, 1H, Si−H), 4.96 (m, 4H, −CH=CH$_2$), 5.80 (tdd, J = 6.7, 10.2 and 16.9 Hz, 2H, −CH=CH$_2$). ^{13}C NMR (75 MHz, CDCl$_3$): δ (ppm) −5.87 (Si−CH$_3$), 13.14 (Si−CH$_2$), 24.89 (Si−CH$_2$−CH$_2$), 29.34 (−CH$_2$−), 29.54 (−CH$_2$), 29.74 (−CH$_2$), 29.91 (−CH$_2$−), 33.67 (−CH$_2$−), 34.20 (−CH$_2$−CH=CH$_2$), 114.45 (−CH=CH$_2$), 139.46 (−CH=CH$_2$). ^{29}Si NMR (80 MHz, CDCl$_3$): δ (ppm) −9.7. IR (characteristic absorption bands): Q (cm^{-1}) 2101 (stretching Si−H mode), 1639 (stretching C=C mode), 1248 (stretching Si−CH$_3$ mode).

Anionic Polymerization. (a) Poly[(ethylene oxide)-b-(allyl glycidyl ether)] and poly[(allyl glycidyl ether)-b-(ethylene oxide)-b-(allyl glycidyl ether)]. The macroinitiator (5 g, 1 mmol monomethoxy-PEO with 5000 g/mol) was dissolved in 20 mL of benzene to give a 20 wt % solution. Cesium hydroxide (134 mg, 0.8 mmol, i.e., 80% deprotonation) was added under argon atmosphere. Stirring at 60 °C for 30 min and evacuation at 90 °C to remove the reaction water for 2 h produced the cesium alkoxide, which was allowed to cool to room temperature. Subsequently, the calculated amount of freshly distilled allyl glycidyl ether in dry toluene (ca. 50 wt %) was added with a syringe (for a DP$_n$ of 20, 2.3 g, 20 mmol in 2.5 mL of toluene). The mixture was stirred for 30 min at room temperature, and polymerization was carried out for 24 h at 90 °C in vacuo. The polymerization was terminated by addition of an excess of methanol (ca. 5 mL) and acidic ion-exchange resin. Filtration and precipitation in cold diethyl ether resulted in the pure polymer. ^{1}H NMR (300 MHz, CDCl$_3$) δ [ppm]: 5.87 (O−CH$_2$−CH=CH$_2$); 5.19 (O−CH$_2$−CH=CH$_2$); 3.97 (O−CH$_2$−CH=CH$_2$); 3.78−3.36 (O−CH$_x$−: PEO, backbone). SEC-RI (THF): 1, M_n = 7700, D = 1.08; 11, M_n = 2950, D = 1.10; 17, M_n = 9300, PDI = 1.05.

Hydrosilylation Polyaddition. (a) In batch: 200 mg of the PEO-PAGE diblock or triblock copolymer was placed in a Schlenk flask and heated to 60 °C in vacuo for 1 h to remove any traces of residual solvents. The flask was backfilled with dry argon, 100 μL of dry chlorobenzene and the calculated amount of monomer (e.g., 100 mg for **2**, i.e., 1:1 core double bonds to silane monomer) were added with a syringe. After formation of a homogeneous solution, 5 μL of Karstedt catalyst solution was added and the reaction was

Table 1. Size Exclusion Chromatography (SEC), Multi-Angle Light Scattering (MALLS) Data for all Linear-Hyperbranched AB-Type Diblock Copolymers

		SEC[a]		MALLS[a]	
		M_n	PDI	M_n	PDI
1	PEO$_{113}$-PAGE$_{30}$	7700	1.08	8400	1.05
2	PEO$_{113}$-(PAGE$_{30}$-*hb*-MDUS$_{21}$)	9770	1.10	15900	1.15
3	PEO$_{113}$-(PAGE$_{30}$-*hb*-MDUS$_{48}$)	11500	1.35	25200	1.30
4	PEO$_{113}$-(PAGE$_{30}$-*hb*-MDUS$_{87}$)	12600	1.40	39000	1.35
5	PEO$_{113}$-(PAGE$_{30}$-*hb*-MDUS$_{91}$)	14600	1.09	40100	1.14
6	PEO$_{113}$-(PAGE$_{30}$-*hb*-MDAS$_{13}$)	10900	1.27	10000	1.21
7	PEO$_{113}$-(PAGE$_{30}$-*hb*-MDAS$_{39}$)	13900	1.17	13300	1.13
8	PEO$_{113}$-(PAGE$_{30}$-*hb*-MDAS$_{51}$)	14700	1.16	14800	1.14
9	PEO$_{113}$-(PAGE$_{30}$-*hb*-MDAS$_{83}$)	16700	1.24	18800	1.27
10	PEO$_{113}$-(PAGE$_{30}$-*hb*-MDAS-Ph$_{83}$)	14300	1.16	23200	1.20
11	PEO$_{17}$-PAGE$_{19}$	2950	1.10	3200	1.09
12	PEO$_{17}$-(PAGE$_{19}$-*hb*-MDAS$_{17}$)	4700	1.14	5200	1.13
13	PEO$_{17}$-(PAGE$_{19}$-*hb*-MDAS$_{30}$)	6450	1.41	6800	1.32
14	PAGE$_{25}$	2900	1.10	3100	1.10
15	PAGE$_{25}$-*hb*-MDAS$_{35}$	7300	1.38	8800	1.32
16	PAGE$_{25}$-*hb*-MDUS$_{39}$	12300	1.29	16800	1.38

[a] PDI = polydispersity index; measurements were performed in THF as an eluent.

continued until disappearance of the Si−H signal in the IR-spectrum (usually 5−10 h). The mixture was cooled to room temperature and separated from undesired carbosilane homopolymer by flash chromatography using first petroleum ether as an eluent, followed by chloroform to elute the product (yields 40−90%). Molecular weights and polydispersities can be found in Table 1.

^{1}H NMR (300 MHz, CDCl$_3$) δ [ppm]: 6.15 (O−C*H*=CH−CH$_3$); 5.91 (O−CH$_2$−C*H*=CH$_2$); 5.76 (−C*H*=CH$_2$); 5.36 (−C*H*=C*H*−); 5.28−5.04 (O−CH$_2$−CH=C*H$_2$*); 5.03−4.82 (−CH=C*H$_2$*); 4.80−4.60 (O−CH=C*H*−CH$_3$); 3.94 (O−C*H$_2$*−CH=CH$_2$); 3.87−3.15 (O−C*H$_x$*−: PEO, backbone); 1.99 (−C*H$_2$*−CH=CH$_2$); 1.69−1.41 (O−CH$_2$−C*H$_2$*−); 1.41−1.02 (C*H$_2$*); 0.57−0.20 (Si−C*H$_2$*−); −0.12, −0.14 (Si−C*H$_3$*) (for MDUS the signal intensities vary and a greater variety of signals due to isomerized products are found, compare Figures 3 and 4 and Supporting Information.)

(b) Slow monomer addition: the procedure employed is analogous to the previous synthesis, but the monomer was diluted in pentane (ca. 1 g in 500 mL) and slowly added with a syringe pump over a period of 10−20 h, while the low boiling pentane was simultaneously removed by distillation.

Preparation of Samples for Transition Electron Microscopy (TEM). The concentration of the block copolymer samples in aqueous solution was 1 g/L. Samples in diethyl ether were dissolved at a somewhat lower concentration of 0.5 g/L. All TEM samples were prepared in the following manner: The block copolymer (3−5 mg) was dissolved in ca. 50 μL of THF and then diluted with the respective nonsolvent (water or diethyl ether) to induce micellization (concentration was adjusted as mentioned above to give clear to opaque stable solutions). For the aqueous sample, THF was removed under reduced pressure. Samples were drop cast on a copper TEM grid and dried at 40 °C overnight.

Results and Discussion

Hydrosilylation is a high yield reaction, and thus numerous approaches for polymer synthesis relying on hydrosilylation polyaddition have been presented in recent years.[16] In the only work on block copolymers with hyperbranched polycarbosilane block published to date, our group used poly(styrene)-*b*-poly(butadiene) block copolymers with pendant vinyl groups to attach hyperbranched polycarbosilanes.[11] Undesired concurrent homopolymerization of the AB$_2$ monomer to a hyperbranched polycarbosilane could be minimized by using slow-monomer addition, but still presented a problem for the synthesis of the block copolymers. Another approach to reduce undesired homopolymerization and favor attachment to the core molecule is the use of highly reactive functional groups at the B$_f$-type core.[17] This approach has been used by Fossum et al. in elegant work for the synthesis of hyperbranched poly(arylene ether phosphine oxide)s[18] or more recently by Stiriba et al. for the synthesis of hyperbranched poly(glycerol) with a benzophenone core.[19] However, the strategy has not been exploited for a polymer core to date. In the current work we capitalize on the enhanced reactivity of allyloxy groups of poly(allyl glycidyl ether) in hydrosilylation reactions in comparison to the less activated alkenylsilanes. In this manner a highly reactive polymer core is combined with AB$_2$-monomers of moderate reactivity for the hypergrafting procedure. This is intriguing with respect to the following questions: (i) Can the growth of the hyperbranched PCS block at a suitable AB- or ABA-block copolymer structure be controlled? (ii) Can slow monomer addition be avoided due to the high reactivity of the core?

A. Synthesis of Linear-Hyperbranched Block Copolymers. Catalytic hydrosilylation polymerization has been employed for the generation of the hyperbranched block via "hypergrafting" of the branched polycarbosilane block onto anionically synthesized poly(ethylene oxide)-*b*-poly(allyl glycidyl ether) di- and triblock copolymers (PEO$_{113}$-*b*-PAGE$_{30}$ (**1**), PEO$_{17}$-*b*-PAGE$_{19}$ (**11**), and PAGE$_{10}$-*b*-PEO$_{136}$-*b*-PAGE$_{10}$) (**17**)), respectively, which represent the macromolecular "core structures" in the syntheses. Diallyl(methyl)silane (MDAS) and methyldiundec-10-enylsilane (MDUS) were employed as the respective AB$_2$-monomer structures with different reactivity in the hydrosilylation polyaddition leading to the hyperbranched block. Different ratios of AB$_2$-monomer to polymer core functionalities were employed in order to vary the molecular weights of the resulting

Scheme 2. Reaction Scheme for the Synthesis of Linear-Hyperbranched Poly(ethylene oxide)-*b*-poly(carbosilane) Amphiphilic Block Copolymers

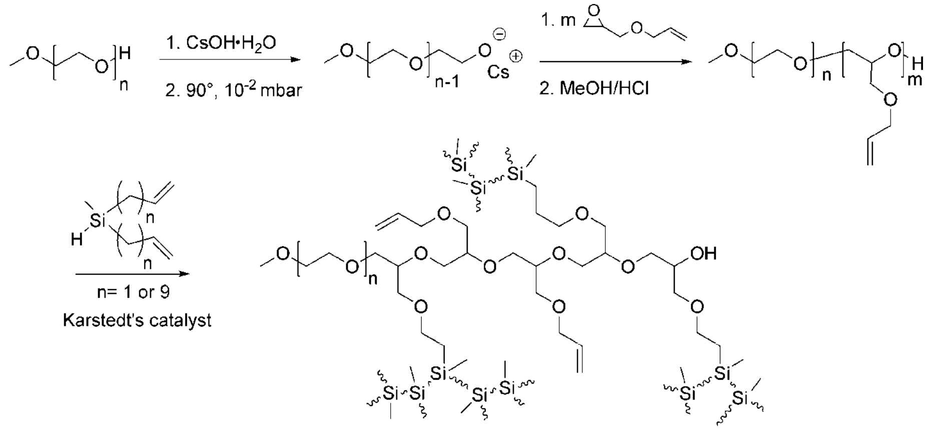

Table 2. Size Exclusion Chromatography (SEC), Multi-Angle Light Scattering (MALLS) Data for the Linear-Hyperbranched ABA Type Triblock Copolymers

		SEC[a]		MALLS[a]	
		M_n	PDI	M_n	PDI
17	$PAGE_{10}$-PEO_{136}-$PAGE_{10}$	9300	1.05	10400	1.03
18	PEO_{136}-$[(PAGE_{10}$-*hb*-$MDUS)_{15}]_2$	8600	1.20	12300	1.15
19	PEO_{136}-$[(PAGE_{10}$-*hb*-$MDUS)_{35}]_2$	11300	1.07	21700	1.07
20	PEO_{136}-$[(PAGE_{10}$-*hb*-$MDUS)_{40}]_2$	11900	1.10	23100	1.08
21	PEO_{136}-$[(PAGE_{10}$-*hb*-$MDUS)_{105}]_2$	12400	1.48	46000	1.88
22	PEO_{136}-$[(PAGE_{10}$-*hb*-$MDAS)_{15}]_2$	10300	1.12	12400	1.10
23	PEO_{136}-$[(PAGE_{10}$-*hb*-$MDAS)_{24}]_2$	12600	1.17	16000	1.18
24	PEO_{136}-$[(PAGE_{10}$-*hb*-$MDAS)_{38}]_2$	15400	1.18	19800	1.14

[a] PDI = polydispersity index; measurements were performed in THF as an eluent.

copolymers. The synthetic strategy for the synthesis of the linear-hyperbranched diblock and triblock copolymers is shown in Scheme 2. Anionic ring-opening polymerization of allyl glycidyl ether onto a living PEO-anion directly produces the macro-core for the ensuing hydrosilylation reaction with the di(alkenylsilane) monomers. Employing cesium counterions, as reported recently for another class of structurally related polyether block copolymers,[11] polymerization proceeds in a living manner and produces the linear block-copolymer precursor in quantitative yield and low polydispersity (<1.1).[20]

It is important to point out that the pendant allyloxy groups at the linear poly(allyl glycidyl ether) block are very reactive in platinum-catalyzed hydrosilylation reactions because of fast and efficient addition to the metal center due to a chelating effect of the oxygen atom and its high energy HOMO.[21] In addition, from a theoretical point of view the high concentration of double bonds (cf. Tables 1 and 2) in the linear block copolymer cores is expected to lead to low polydispersity materials. Indeed, detailed NMR-studies (*vide infra*) demonstrate that the entire polymer core is incorporated in the final polymer, and—as expected—no unreacted linear block copolymer precursor can be found in the reaction mixture, when all silane monomer is consumed (compare Figures 1 and 2). In contrast, the allyl and undecenyl groups of both carbosilane AB_2-monomers are of moderate reactivity in a hydrosilylation reaction. In the case of MDUS the long alkyl chains were expected to render intramolecular cyclization less probable, but simultaneously lower the reaction rate of the hydrosilylation for steric reasons. MDAS with its shorter alkyl chains represents an interesting monomer structure, since the short C_3-segment between the silicon centers permits detailed characterization of the branched architecture via ^{29}Si NMR-spectroscopy.[1,2]

We also prepared a PAGE homopolymer (entry **14** Table 1) and used it as a core for the hypergrafting hydrosilylation. The resulting hypergrafted homopolymer may be viewed as a statistically branched analogue of the structurally perfect dendronized polymers[22] that have been reported in literature.[23] Recent results by Twyman and co-workers[24] demonstrated broad molecular weight distributions (>2) for randomly hypergrafted polymers. However, in this work the separation of the desired “hypergrafted” polymer from concurrently formed hyperbranched homopolymer was neglected. Interestingly, in our case the carbosilane homopolymer can be separated from the hypergrafted product via flash-chromatography in the described manner. After the separation two copolymers (**15** and **16**) with moderate polydispersity were obtained.

SEC analysis of the crude reaction product (Figure 1) shows a bimodal molecular weight distribution. Besides the narrow mode of the linear-hyperbranched block copolymer a second, broad distribution mode can be observed at lower molecular weight. The undesired broad low molecular weight fraction with a polydispersity M_w/M_n exceeding 2 corresponds to homopolymerization of AB_2-monomers via a conventional step-growth mechanism. This pathway generates low molecular weight hyperbranched homopolymer, which is not attached to the growing branched diblock structure, possibly due to cyclization via reaction of the focal Si−H group with one of the allyl end groups. In the case of MDUS this homopolymer fraction may even possess similar molecular weight as the targeted block copolymer. However, due to the different solubility characteristics of both blocks, the nonattached hyperbranched polycarbosilane homopolymer can be conveniently separated from the desired block copolymer by silica column chromatography, as it is obvious from TLC experiments (Figure 1, right). In the first step of the flash-chromatography, the undesired *homo*-poly(carbosilane) is removed by elution with petroleum ether, which is a nonsolvent for PEO, but an excellent solvent for the apolar hyperbranched PCS (compare Figure 1, left). Subsequently the linear-hyperbranched block copolymer is eluted with a mixture of chloroform: methanol (3:1). After fractionation, a monomodal molecular weight distribution with narrow poly-

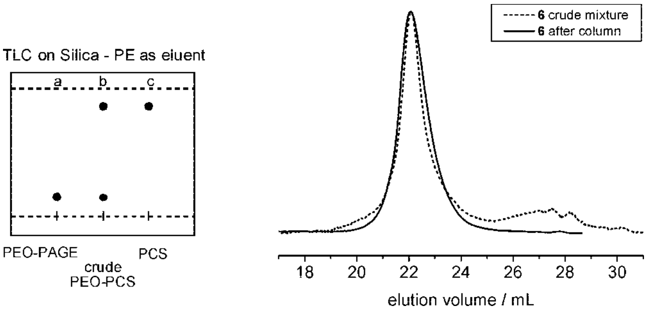

Figure 1. Left: thin layer chromatography of (a) linear precursor (PEO-PAGE), (b) crude reaction mixture (crude PEO-PCS), and (c) homo poly(carbosilane) (PCS). Right: size exclusion chromatogram in THF, comparison between crude reaction mixture and linear-hyperbranched polymer **6** after separation from homopolymer (PE = petroleum ether).

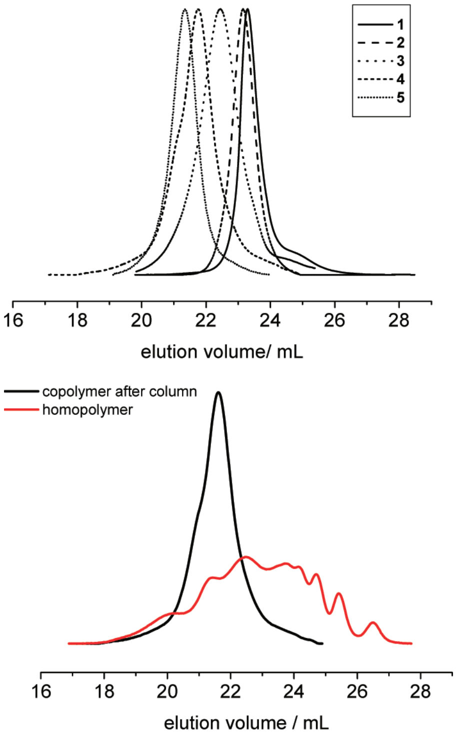

Figure 2. Top: SEC traces of linear precursor and linear-hyperbranched block copolymers (samples **1**−**5**) based on MDUS. Bottom: Comparison of both fractions (homopolymer, diblock copolymer) after fractionation by flash-chromatography.

dispersity in SEC is obtained (Figure 1). Comparing both AB_2-monomers employed, MDAS shows a higher tendency for homopolymerization due to faster reaction kinetics compared to MDUS with the long alkyl chains that lower the rate of cyclization. Table 1 summarizes the molecular weight data of the block copolymers obtained by size exclusion chromatography (SEC) combined with multiangle laser light scattering (MALLS). Clearly, the amount of the AB_2-carbosilane monomer added depends on the targeted molecular weight of the hyperbranched block.

B. Molecular Characterization of the Linear-Hyperbranched Block Copolymers. For all linear-hyperbranched hybrid block copolymers rather narrow molecular weight distributions have been obtained in SEC (PDI in the range of 1.10−1.40, cf. Figures 1 and 2). The block copolymers were analyzed with SEC-RI and MALLS (multiangle laser light scattering) detection, revealing a large difference in apparent molecular weight (compared to polystyrene standards) and absolute molecular weight (determined via MALLS). Due to their rather globular and compact structure, (hyper)branched polymers elute at higher elution volumes, which leads to a decrease of the apparent molecular weight in SEC[25] (a comparative plot of both detector signals can be found in the Supporting Information). Using light-scattering, absolute molar masses obtained for the copolymers are always significantly higher than the values determined via SEC. This effect is particularly pronounced for copolymers with MDUS-based carbosilane block (cf. entries **2**−**5** and **18**−**21** in Tables 1 and 2).

Molecular masses of the diblock copolymers can reach high values, when MDUS is used, while the molecular weight in the case of MDAS as a monomer is rather limited, which may be due to this monomer's stronger tendency to both homopolymerize (and cyclize), limiting the fraction of monomer available for hypergrafting. Nevertheless, the maximum degree of polymerization achieved for both monomers is similar (90−100 units). A higher ratio of monomer:core results in an increasing extent of homopolymerization, limiting the degree of hypergrafting.

In order to demonstrate the possibility of further functionalization of the branched block, sample (**10**) was reacted with dimethylphenylsilane in order to end-cap all terminal double bonds of the PCS-block. As another modification of the reaction conditions, a second diblock copolymer with a short PEO block was used and reacted with MDAS (PEO_{17}-$PAGE_{19}$, **11**). Two different molecular weights were targeted and narrow molecular weight distributions were obtained (M_n 5200, PDI 1.13 (**12**) or M_n 6800, PDI 1.32 (**13**)).

Generally, detailed SEC investigation revealed that slow monomer addition in the current case offered no advantages concerning the degree of hypergrafting compared to the more convenient batch copolymerization of the AB_2 carbosilane monomers. In the case of MDUS, we assume that this is in part due to pronounced isomerization of the terminal double bonds in the case of slow monomer addition to internal double bonds, which are no longer reactive in a further hydrosilylation polyaddition. This phenomenon becomes increasingly dominant, when slow monomer addition is applied—usually over a period of 24 h or more—because the reaction time of the catalyst with the growing macro-core is considerably longer than in a bulk reaction. The active catalyst will then cause undesired side reactions, like double bond isomerization or coupling reactions. If a large amount of monomer is present (like in the bulk reaction) these side reactions still occur, but are less pronounced.

ABA-Type Linear-Hyperbranched Triblock Copolymers. The synthesis of ABA-type hyperbranched-linear-hyperbranched triblock copolymers was carried out using the linear ABA-triblock copolymer $PAGE_{10}$-PEO_{136}-$PAGE_{10}$ (sample **17**). **17** was synthesized in complete analogy to the diblock copolymer, however, a commercial dihydroxyfunctional PEO with a molecular weight of 6000 g/mol (DP_n = 136) was used as macroinitiator for the anionic ring-opening polymerization of allyl glycidyl ether. The length of the PAGE-blocks targeted was 10 repeating units on each side of the PEO-block. It is reasonable to assume that each A-block of the macroinitiator and the resulting ABA-triblock core possesses similar reactivity and thus the proposed, symmetric triblock architecture is achieved after hydrosilylation with the AB_2 monomers. The hypergrafting reaction was carried out in the same manner as for the diblock copolymer synthesis (*vide supra*). In contrast to the AB-diblock copolymers, purification of the linear-hyperbranched triblock copolymers via silica chromatography was impeded by good solubility of the ABA structures in petroleum ether. A fraction of the ABA structures appears to be trapped in the PCS homopolymer and therefore is eluted together in petroleum ether (as determined gravimetrically ca. 10−20%). Still, the purified block copolymer fraction can be recovered after solvent exchange with the more polar eluent ($CHCl_3$/MeOH). Data for ABA-structures are summarized in Table 2. The slightly higher polydispersity in the case of **21** found via MALLS may be explained by side reactions that may occur in hydrosilylation reactions of long chain alkenylsilanes (e.g., coupling, cross-linking, etc.). Nevertheless, the coupled amount can be seen to be negligible, as SEC characterization gave a rather narrow molecular weight distribution.

Detailed NMR Characterization and Degree of Branching DB. In general, the ^1H NMR spectra of the linear-hyperbranched block copolymers are rather complicated due to the complex structure of the hypergrafted block. Nevertheless, detailed information on the polymer structure can be extracted. Isomerization of both kinds of double bonds both (a) at the backbone and (b) in the periphery of the PCS block is observed (cf. Figure 3 and Supporting Information). However, in the case of MDAS

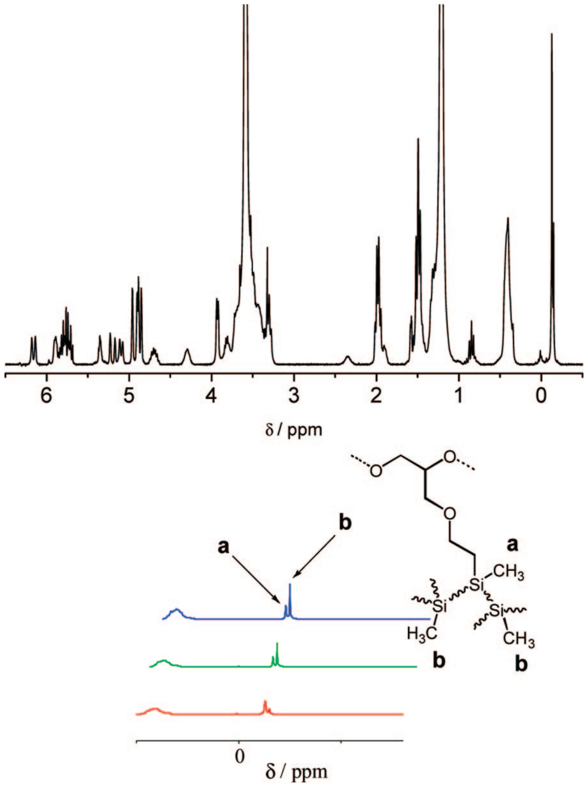

Figure 3. Top: ^1H NMR ($CDCl_3$) of (**2**). Bottom: silane region of proton NMR of linear-hyperbranched diblock copolymers (**2**, **3**, **4**) evidencing growth of the hyperbranched block.

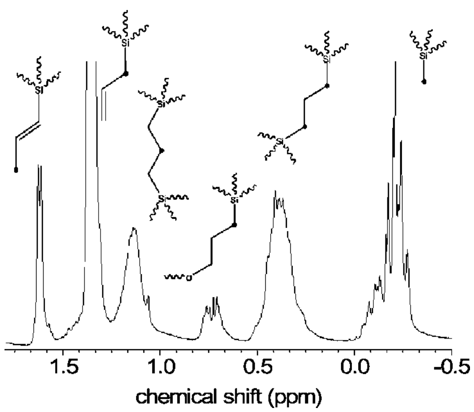

Figure 4. Silane region of the ^{1}H NMR spectrum of linear-hyperbranched diblock copolymer **7**, showing different methylene signals in the branched structure.

the different methylene signals close to 0 ppm can be analyzed separately. The spectra permit detailed characterization of the extent of reaction of the allyl groups of the core. Clearly for MDUS incomplete reaction of the core functionalities is observed. This is most probably due to steric reasons, i.e., not every pendant allyl group in the core is accessible for the bulky MDUS monomer after attachment of the first carbosilane monomers. A conversion of approximately 30−40% of the double bonds of the polymer core can be estimated from the spectra.

In pronounced contrast, for MDAS all allyl groups along the backbone can react with the AB_2-monomer, but a stoichiometric excess is necessary, since even at a composition of 1:1 (carbosilane: core-double bonds) a branched structure is obtained and some of the core double bonds remain unreacted. A small signal can be assigned at 6.00 ppm that is due to isomerized core-vinyl ethers (compare Supporting Information).

Unfortunately, it is not possible to determine molecular weights independently from ^{1}H NMR spectra because of strong overlap of the resonances; the single methoxy end group of the linear PEO segment cannot be discerned. Nevertheless, it can be directly recognized in the spectra that the molecular weight of the hyperbranched block increases with increasing monomer: core ratio, as the integral intensity of the PCS signal rises. This corresponds to the previously discussed SEC and MALLS data, keeping in mind that the PCS homopolymer has been removed prior to characterization.

For the case of MDUS one can easily distinguish between monomers that are directly attached to the backbone and monomers that are attached in the periphery, when zooming into the silane region of the ^{1}H NMR or in the ^{29}Si NMR spectrum (Figure 3, top, shows the ^{1}H NMR spectrum of sample **2** and right the enlarged region for samples **2**, **3**, and **4**; the corresponding ^{29}Si NMR data can be found in the Supporting Information). In the ^{1}H NMR spectrum the signal at higher field (−0.09 ppm) is assigned to the Si−Me-groups in the periphery of the hyperbranched polycarbosilane, while the signal at lower field (−0.07 ppm) is assigned to the Si−Me-signal of monomers directly linked to the polyglycerol core. In addition, the ^{29}Si spectrum shows two different resonances at 3.5 and 2.9 ppm for the two possible environments bound in the periphery or directly to the core, respectively. The latter are still affected by the electron withdrawing effect of the allyloxy group, thereby shifting the signal to slightly lower field. As one can observe two different signals even for a composition of 1:1 (double bonds core vs carbosilane functionality), definite proof for a hyperbranched structure and not a mere linear functionalization of the PEO-PAGE block copolymer is obtained. This is also in agreement with the underestimation of molecular weights in SEC measurements as expected for hyperbranched materials. When MDAS is used as a monomer one can distinguish all methylene signals of the hyperbranched PCS structure (Figure 4, signal assignment was achieved by simulation using ACD NMR Version 9 and estimation of the respective electron densities at the protons).

From a theoretical point of view six different modes of monomer incorporation are possible, resulting from reaction of the core allyloxy units as well as from the hyperbranched polycarbosilane structure. In the ^{29}Si NMR spectrum of the polymers all different silicon environments within the branched polymer structure lead to different chemical shifts, as shown in

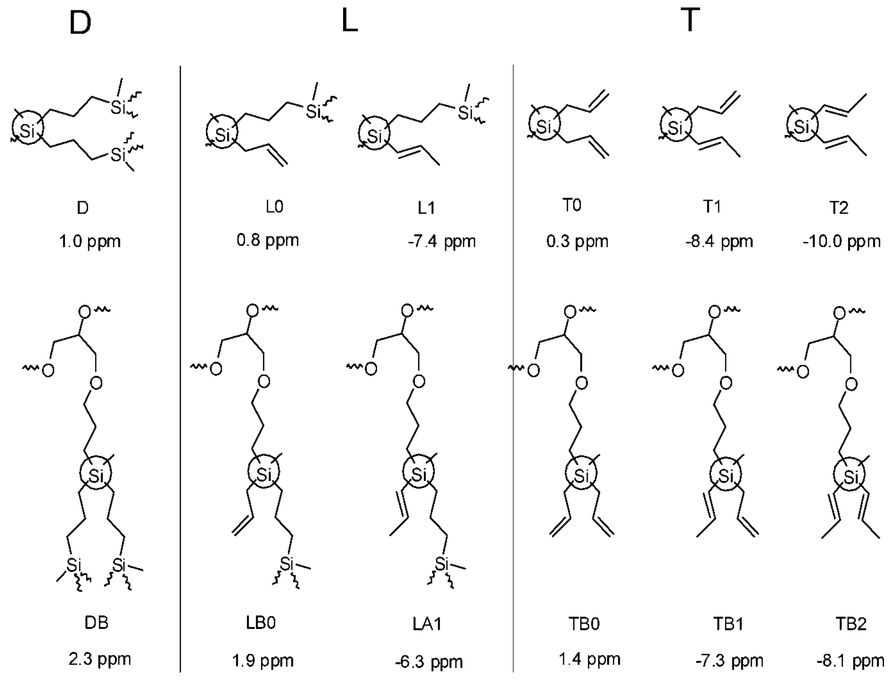

Figure 5. ^{29}Si NMR shifts for PEO$_n$-(PAGE$_{30}$-*hb*-MDAS$_n$) in $CDCl_3$. Different Si environments can be distinguished. (Signal assignment was made in analogy to the literature.[26])

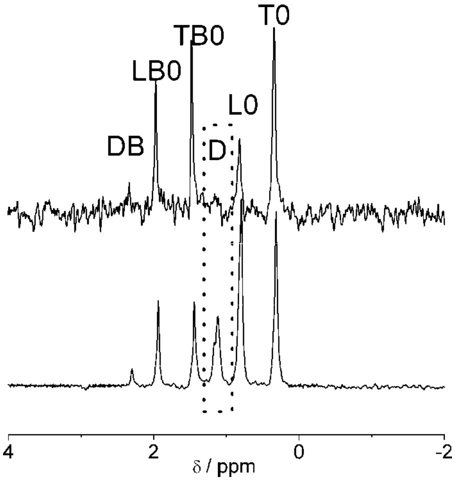

Figure 6. ^{29}Si NMR spectra of polymers **12** (top) and **13** (bottom) showing an increasing fraction of dendritic Si-centers in the hyperbranched polycarbosilane upon increasing the amount of AB$_2$-monomer (for abbreviations cf. Figure 5).

Table 3. Thermal Characterization Obtained via Differential Scanning Calorimetry (DSC) Data for the Linear-Hyperbranched AB and ABA Block Copolymers with a Crystalline Segment

		T_g[a]	T_m[a]	ΔH[a]	topology
1	PEO$_{113}$−PAGE$_{30}$	−74	59	69	*l*-AB
2	PEO$_{113}$-(PAGE$_{30}$-*hb*-MDUS$_{21}$)	−71	58	51	*hb*-AB
3	PEO$_{113}$-(PAGE$_{30}$-*hb*-MDUS$_{48}$)	−71	57	36	*hb*-AB
4	PEO$_{113}$-(PAGE$_{30}$-*hb*-MDUS$_{87}$)	−71	57	28	*hb*-AB
5	PEO$_{113}$-(PAGE$_{30}$-*hb*-MDUS$_{91}$)	−72	50	22	*hb*-AB
6	PEO$_{113}$-(PAGE$_{30}$-*hb*-MDAS$_{13}$)	−76	46	52	*hb*-AB
7	PEO$_{113}$-(PAGE$_{30}$-*hb*-MDAS$_{39}$)	−76	46	42	*hb*-AB
8	PEO$_{113}$-(PAGE$_{30}$-*hb*-MDAS$_{51}$)	−77	45	36	*hb*-AB
9	PEO$_{113}$-(PAGE$_{30}$-*hb*-MDAS$_{83}$)	−76	43	30	*hb*-AB
17	PAGE$_{10}$-PEO$_{136}$−PAGE$_{10}$	−69	47	67	*l*-ABA
18	PEO$_{136}$-[(PAGE$_{10}$-*hb*-MDUS)$_{15}$]$_2$	−74	52	50	*hb*-ABA
19	PEO$_{136}$-[(PAGE$_{10}$-*hb*-MDUS)$_{35}$]$_2$	−77	47	44	*hb*-ABA
20	PEO$_{136}$-[(PAGE$_{10}$-*hb*-MDUS)$_{40}$]$_2$	−76	45	39	*hb*-ABA
21	PEO$_{136}$-[(PAGE$_{10}$-*hb*-MDUS)$_{105}$]$_2$	−77	41	23	*hb*-ABA
22	PEO$_{136}$-[(PAGE$_{10}$-*hb*-MDAS)$_{15}$]$_2$	−75	34	52	*hb*-ABA
23	PEO$_{136}$-[(PAGE$_{10}$-*hb*-MDAS)$_{24}$]$_2$	−72	30	44	*hb*-ABA
24	PEO$_{136}$-[(PAGE$_{10}$-*hb*-MDUS)$_{38}$]$_2$	−70	25	36	*hb*-ABA

[a] Determined via DSC of a preheated sample at a heat rate of 5 K/min. T_g = glass transition temperature in °C (± 1,5 °C). T_m = melting point in °C (± 1,5 °C). ΔH = melting enthalpy in J/g; estimated error ± 1.5 J/g.

Figure 5. Dendritic (D), terminal (T), and linear units (L) can be assigned unambiguously both in the PCS-periphery or directly linked to the PAGE-core. Additionally, different signals for isomerized double bonds can be found at higher field.

Figure 6 shows a comparison of the polymers **12** and **13**, revealing an increasing amount of peripheral dendritic units and a higher DB, which is clearly a consequence of an increasing fraction of AB$_2$-monomer attached. The ^{29}Si NMR shift at 1.0 ppm corresponds to these silicon centers (complete ^{29}Si NMR spectrum including also the isomerized signals can be found in the Supporting Information).[26] The overall degrees of branching of the hypergrafted block can be estimated from the ^{29}Si NMR spectra and vary between 30 and 45%. For hyperbranched blocks with elevated molecular weights (e.g., entries **8**, **9**, **24**) these values are very close to the theoretical maximum degree of branching for the batch procedure (50% is predicted for AB$_2$-systems).[17,27]

C. Thermal Properties and Solution Structures. *Thermal Behavior.* The key questions to be addressed in this final section are as follows: (i) How does the hyperbranched polycarbosilane block influence crystallization of the PEO block? (ii) Does the amphiphilicity of the materials in combination with the unusual polymer architecture permit micellization in solution? (iii) Is there a peculiar impact of the highly branched topology on association in solution? It should be emphasized that, e.g., in contrast to PEO-PAMAM block copolymers with PAMAM dendrimer block presented by Hammond et al.,[28] the hyperbranched segment represents the majority phase, which is usually not possible when dendrimers are involved in the synthesis that possess commonly rather low molecular weight even in generation 4.

DSC measurements of all hybrid copolymers have been performed (cf. Table 3). All materials showed glass transitions (T_g) in the range of −77 to −69 °C, typical of the flexible hyperbranched polycarbosilane block. In the case of block copolymers with longer PEO segments (DP$_n$ = 113 and 136, respectively) not only the T_g of the PCS block is observed, but also a melting endotherm for the linear PEO block in the range of 43 to 60 °C. Even for sample **4** with only 13wt% of PEO a weak melting endotherm was observed, evidencing crystalline PEO domains highly dispersed in the hyperbranched PCS matrix. This evidence in general the expected phase-segregated nature of the block copolymers in bulk and is in clear contrast to the behavior of PEO-*dend*-polybenzylether block copolymers studied by Fréchet et al.,[10c] which exhibit miscibility, if the perfect dendrimer block represents the majority phase. Interestingly, for our materials the melting point of PEO is hardly shifted to lower temperatures, even if the molecular weight of the hyperbranched block increases drastically. This is tentatively explained by the high stability of the crystalline domains of PEO, even upon dilution of these domains in a majority phase of amorphous, hyperbranched PCS.

The melting point of PEO is influenced systematically to a stronger extent, when MDAS is used as branching monomer (T_m = 43−46 °C) than in the case of MDUS (50−58 °C, compare Table 3). This different melting point depression of the crystalline PEO-block must be related to thickness (and stability) of the crystalline lamellae. Obviously, the presence of the longer alkyl chains of the MDUS-units exerts a weaker influence on the crystalline domains via the phase boundary than the short propyl-units in the MDAS-structure. Hammond and co-workers observed a similar depression of the melting point of PEO upon attachment of perfectly branched PAMAM dendrimers to the end group of PEO, which decreased with dendrimer generation from G2 to G5.[28]

The block copolymers with short PEO block (DP$_n$ = 17) do not show crystallization, and only the glass transition temperature of the PCS-block is detected. Unmodified PEO of this molecular weight has a low melting point of ca. 25 °C. Crystallization is obviously suppressed by the amorphous hyperbranched segment, leading to miscibility.

Furthermore, the melting enthalpies ΔH of the crystalline PEO-fraction have been measured and compared. The presence of the linear, amorphous PAGE-block already impedes crystallization of PEO, reducing the melting enthalpy. With increasing molecular weight of the hyperbranched PCS block a further gradual decrease of ΔH is observed, which stems from the decreasing fraction of the linear PEO-component.

For the triblock copolymers the same general trend is observed, resulting in even lower melting points (compare Table 3). Again, the series of block copolymers with the shorter MDAS-segments and therefore higher branch point density generally leads to lower melting points than the long undecenyl chains in the MDUS series. Within the series of block copolymers, an increase of the size of the hyperbranched block led to a systematic decrease of the melting points for both monomers.

A diagram showing the trends for both melting points and melting enthalpies is given in Figure 7. When normalizing the

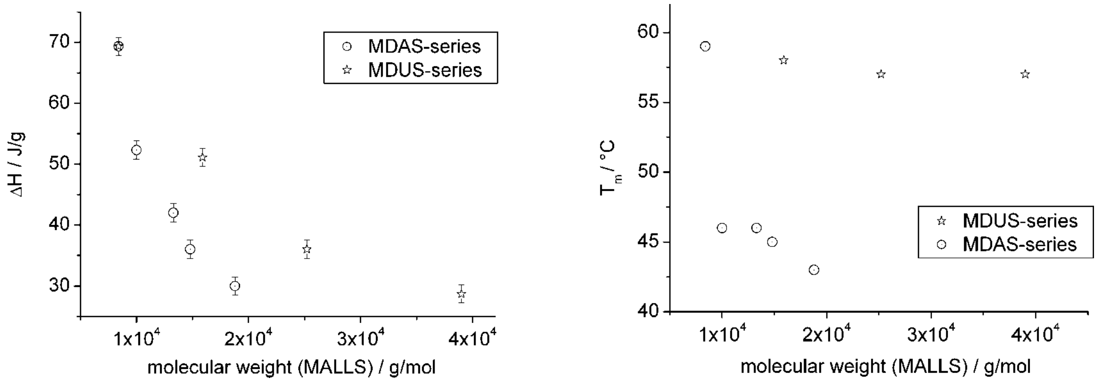

Figure 7. Left: Decrease of the melting enthalpies (ΔH, estimated integration error ± 1.5 J/g) of PEO determined via DSC with increasing molecular weight of the polymers for the series of AB-type diblock copolymers. Right: melting points of the diblock copolymers. (MDAS represents the block copolymers based on methyl diallyl silane, while MDUS presents the series of block copolymers based on methyl diundecenyl silane.)

melting enthalpies to the actual weight fraction of PEO in the samples, similar values ΔH_n are obtained for all samples in the respective series.

Systematically lower values for the melting enthalpies ΔH_n in the MDAS series in comparison to the MDUS series (approximately 65 vs 100 kJ/g) point to a stronger disturbance of the crystalline structure in this case. We tentatively explain this by the stronger segregation in the MDUS-series with the long alkyl chains that lead to a strongly apolar character and high incompatibility with PEO.

It should be mentioned that the attachment of the highly stable hyperbranched polycarbosilane block proved an increased thermal stability for all block copolymers in TGA measurements (see Supporting Information).

Aggregation Behavior in Solution. An intriguing issue in the context of linear-dendritic block copolymers is the influence of the branched topology on association in solution. In the series of the linear-hyperbranched block copolymers prepared, the ratio of linear and hyperbranched segment has been varied in a systematic manner. Here we present the results of a preliminary investigation of the aggregation of the linear-hyperbranched amphiphilic block copolymers in solution. Structure formation has been investigated using transition electron microscopy (TEM). Two solvents with different polarity have been used for the micellization process: (i) water as a good solvent for PEO and (ii) diethyl ether as a precipitant for PEO, but as a good solvent for the highly apolar, hyperbranched PCS block.

Only the polymers **2**, **6**, and **7** were readily soluble in aqueous solution, surprisingly even with a rather large weight percentage of the hydrophobic polycarbosilane block (e.g., sample **2** consists of ca. 50 wt % PCS). In their study on perfect carbosilane dendrimers with PEO block, Kim et al. reported water solubility only for [G-1] ($M_n = 195$ g mol^{-1}, 19.3% PCS of copolymer) and [G-2] ($M_n = 673$ g mol^{-1}, 45.2% PCS of copolymer), however, using a low molecular weight PEO of molecular weight of 815 g/mol.[14] Additionally, these authors only reported micellization in water, but no information on inverse micelle formation in a good solvent for the dendritic block or peculiar micelle shapes due to the dendrimer architecture was reported.

Preliminary experiments concerning solvent-induced association of the amphiphilic linear-hyperbranched block copolymers with a high content of hyperbranched segments have been carried out via transmission electron microscopy (TEM) in water (for **2**, **7**, **8**, and **18**) as a solvent for the PEO block as well as diethyl ether. These studies demonstrate a rich variety of supramolecular aggregates, most probably governed both by crystallization of the PEO-block as well as the spatial requirements of the isotropic hyperbranched PCS block. The polymers with larger amount of PCS did not form stable solutions in water, but usually precipitated within minutes. Therefore diethyl ether was chosen as a nonsolvent for PEO, but as a good solvent for the PCS block. TEM images were taken with unstained samples, relying on the contrast due to the silicon atoms and the invisibility of PEO in TEM measurements. Thus, only the silicon-containing domains of the samples are visible in the images shown. As a consequence of the variation of the block length ratio, the morphology of the aggregates also varied drastically with increasing molecular weight of the hyperbranched block (a preliminary overview of the morphologies and tentative structural models are presented in the Supporting Information).

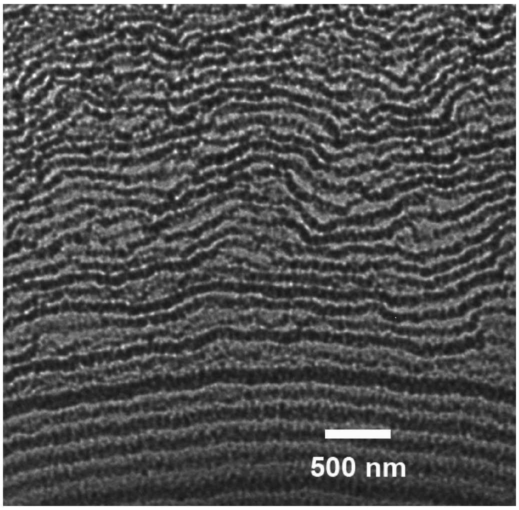

Figure 8. Transition electron microscopy image of linear-hyperbranched diblock copolymer sample **2** PEO_{113}-($PAGE_{30}$-*hb*-$MDUS_{21}$), obtained from aqueous solution (drop casting and drying at 40 °C). Dark domains are Si-rich and thus due to the hyperbranched polycarbosilane.

Figure 8 shows both ordered and disordered lamellar structures that were obtained upon drying of an aqueous solution of polymer **2** (concentration 1 g/L) with approximately 45 wt % PCS. The structure was obtained after slow evaporation of water at 40 °C overnight. The distance between the silicon-containing dark lamellae is estimated to be 60−80 nm. The formation of lamellar order is in line with expectation for the composition of the block copolymers. The disorder of the lamellae may be both due to structural polydispersity of the hyperbranched block with its random branching pattern, but may also be related to the simple drop-casting preparation applied. Undulated bulk morphologies were also reported for the system poly(styrene)-*b*-(poly(carbosilane)).[11,26] When the same sample **2** is dissolved in diethyl ether, rodlike micellar structures with short rod length are observed (not shown). In this case the solution structure is quenched due to fast evaporation of the solvent.

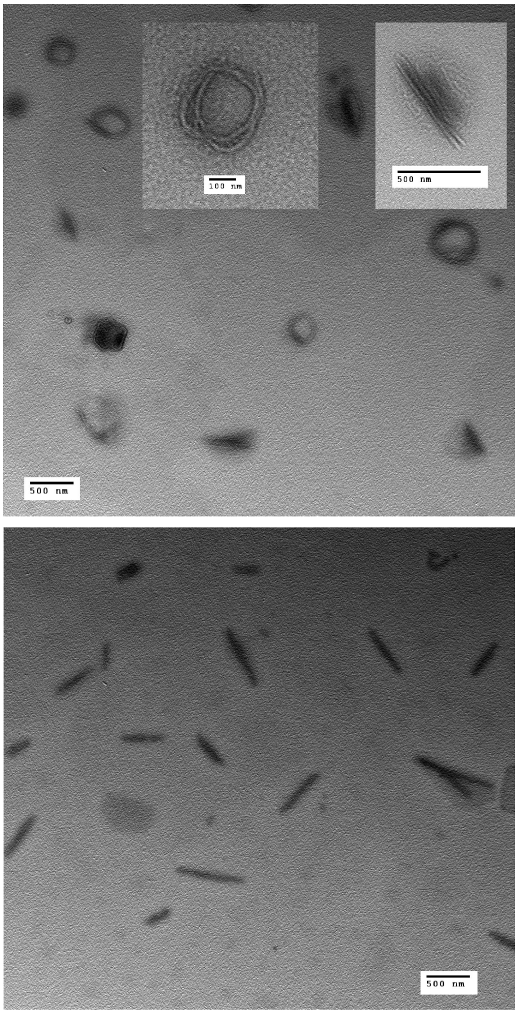

Figure 9. Transition electron microscopy images of the linear hyperbranched diblock copolymers. Top: drop cast sample **3** in diethyl ether. Bottom: drop cast sample **4** in diethyl ether.

If the fraction of the *hb*-polycarbosilane block is further increased (sample **3**, 68 wt % PCS), the polymer becomes insoluble in water. In diethyl ether, however, unusual rodlike aggregates can be observed that vary in their dimensions. The anisotropic aggregates tend to dimerize and may even aggregate into small twisted structures, which are considerably longer than those found for polymer **2** (approximately 400 nm for **3**; Figure 9 left). The diameter of the rods is in the range of 20−25 nm. We assume that both linear and twisted structures are in equilibrium. However, further studies of the solution self-assembly are in progress to confirm this.

Polymer **4** with approximately 80 wt % of PCS forms even longer, nontwisted rods with a length up to 500 nm, which are presumably held together by the crystalline PEO lamellae (Figure 9, right). Interestingly, an enlargement of the TEM-image of the micelles reveals a substructure with a silicon-rich corona. This indicates that the rodlike structures consist of two layers of polymer. Polymer **5** with the highest amount of PCS (87 weight %) formed only spherical micelles under these conditions.

Amphiphilic block copolymers synthesized with MDAS, resulting in the shorter propyl chains, such as polymer **7**, formed rods in diethyl ether similar to those of polymer **2,** but with a lower length and thickness (Figure 10). On the other hand, the same polymer forms spherical micelles in water. Finally, aggregation of ABA-triblock copolymers has also been investigated. Only polymer **18** formed aggregates in the two solvents readily. Both for water and for diethyl ether spherical aggregates were obtained.

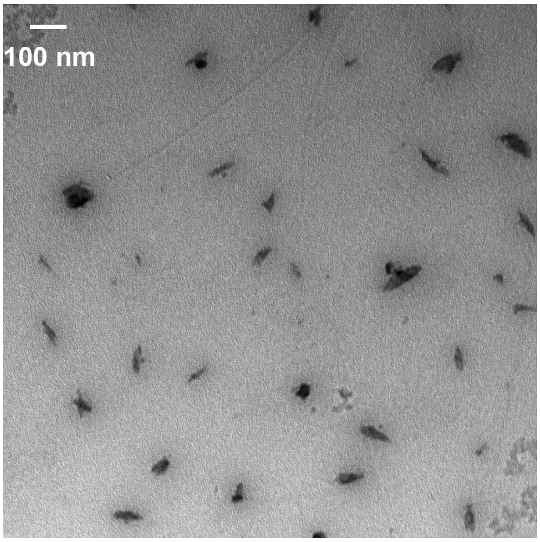

Figure 10. Transition electron microscopy images of the linear-hyperbranched diblock copolymer sample **8** PEO_{113}-($PAGE_{30}$-*hb*-$MDAS_{51}$) in diethyl ether.

Conclusions

We have demonstrated the first controlled synthesis of narrow polydispersity linear-hyperbranched AB and ABA block copolymers with a hydrophilic and crystallizable linear PEO block and a hydrophobic, hyperbranched block consisting of a poly(carbosilane) structure with different alkyl spacer length.

The hypergrafting approach was applied to anionically synthesized poly(ethylene oxide)-*b*-poly(allyl glycidyl ether) AB and ABA-type precursor block-copolymers, using methyldiundec-10-enylsilane (MDUS) or diallyl(methyl)silane (MDAS) as the respective AB_2-monomer for the hydrosilylation polyaddition. With this strategy it was possible to obtain a series of different molecular weights of the hyperbranched block in a facile one-pot hydrosilylation procedure. Due to the high reactivity of the allyloxy groups of the poly(allyl glycidyl ether) segment in hydrosilylation reactions, which permits rapid core-functionalization, slow monomer addition[11] was not necessary and the synthesis was carried out as a simple batch copolymerization. With a convenient purification step the undesired hyperbranched homo-PCS was removed from the linear-hyperbranched block copolymer, relying on flash-chromatography. Pure block copolymers with a well defined, linear, crystalline, water-soluble PEO block and a highly flexible, hydrophobic, hyperbranched polycarbosilane block were obtained. The hyperbranched polycarbosilane block is structurally similar to branched polyethylene linked by flexible carbosilane bridges, possessing a low glass transition temperature. All materials were analyzed using SEC/MALLS- and NMR-methods with respect to molecular weights, polydispersities and the extent of branching. Polydispersities of the block copolymers were in the range of 1.10−1.47, and molecular weights were between 8400 and 40100 g/mol. Furthermore, we have been able to incorporate a homopolymer of allyl glycidyl ether into the hyperbranched architecture with the same approach, yielding statistically dendronized polymers of moderate polydispersity (ca. 1.4).

The thermal properties of the block copolymers reflect strong phase segregation between both blocks as well as enormous stability of the crystalline PEO lamellae. Interestingly, even materials with a large polycarbosilane block remained soluble in water. Unusual rodlike aggregates of these amphiphilic block copolymers formed in solution could be visualized with transition electron microscopy both in water or diethyl ether as solvents for the respective segments.

The nonlinear PEO-PCS block copolymers prepared in this convenient one-pot reaction in 2 steps will broaden the knowledge on linear-hyperbranched systems in general, but also bear promise for a variety of surface and interface applications, since the hyperbranched block can conveniently be functionalized with monofunctional silanes, opening multiple possibilities for attachment of the structures to surfaces or nanoparticles. Cross-linking of the poly(carbosilane) block may result in interesting hydro- and organogels.

Acknowledgment. The authors thank Margarete Deptolla for her technical assistance, Dr. Hannah M. König for TEM measurements and Ursula Grimm, Ulf Herge for TGA measurements. H.F. acknowledges the Fonds der Chemischen Industrie (FCI) for valuable financial support. F.W. is grateful to the graduate class of excellence "POLYMAT" in the context of the graduate school of excellence Mainz for a fellowship.

Supporting Information Available: Figures showing additional NMR data, TGA curves and TEM pictures. This material is available free of charge via the Internet at http://pubs.acs.org.

References and Notes

(1) (a) Feng, X.-S.; Taton, D.; Chaikof, E. L.; Gnanou, Y. *J. Am. Chem. Soc.* **2005**, *127*, 10956–10966. (b) Angot, S.; Taton, D.; Gnanou, Y. *Macromolecules* **2000**, *33*, 5418–5426. (c) Darcos, V.; Duréault, A.; Taton, D.; Gnanou, Y.; Marchand, P.; Caminade, A.-M.; Majoral, J.-P.; Destarac, M.; Leising, F. *Chem. Commun.* **2004**, 2110–2111.

(2) (a) Tomalia, D. A.; Naylor, A. M.; Goddard, W. A. *Angew. Chem.* **1990**, *102*, 138–175. (b) Frey, H.; Lach, C.; Lorenz, K. *Adv. Mater.* **1998**, *10*, 279–293. (c) Bosman, A. W.; Janssen, H. M.; Meijer, E. W. *Chem. Rev.* **1999**, *99*, 1665–1688. (d) Tomalia, D. A. *Adv. Mater.* **1994**, *6*, 529–539.

(3) (a) Yates, C. R.; Hayes, W. *Eur. Polym. J.* **2004**, *40*, 1257–1281. (b) Sunder, A.; Heinemann, J.; Frey, H. *Chem. Eur. J.* **2000**, *6*, 2499–2506.

(4) Kim, Y. H.; Webster, O. W. *Macromolecules* **1996**, *29*, 8583–8586.

(5) (a) Lang, H.; Lühmann, B. *Adv. Mater.* **2001**, *13*, 1523–1540. (b) Frey, H.; Schlenk, C. *Top. Curr. Chem.* **2000**, *210*, 69–129. (c) Majoral, J.-P.; Carminade, A.-M. *Chem. Rev.* **1999**, *99*, 845–880. (d) Frey, H.; Schlenk, H. *Monatsh. Chem.* **1999**, *130*, 3–14. (e) Uchida, H.; Kabe, Y.; Yoshino, K.; Kawamata, A.; Tsumuraya, T.; Masamune, S. *J. Am. Chem. Soc.* **1990**, *112*, 7077–7079. (f) Frey, H.; Lorenz, K.; Mülhaupt, R. *Macromol. Symp.* **1996**, *102*, 19–26.

(6) (a) Xiao, Y.; Wong, R. A.; Son, D. Y. *Macromolecules* **2000**, *33*, 7232–7234. (b) Schlenk, C.; Kleij, A. W.; Frey, H.; van Koten, G. *Angew. Chem., Int. Ed.* **2000**, *39*, 3445–3447. (c) Lach, C.; Frey, H. *Macromolecules* **1998**, *31*, 2381–2383. (d) Whitmarsh, C. K.; Interrante, L. V. *Organometallics* **1991**, *10*, 1336–1344.

(7) (a) Muzafarov, A. M.; Rebrov, E. A.; Gorbacevich, O. B.; Golly, M.; Gankema, H.; Möller, M. *Macromol. Symp.* **1996**, *102*, 35–46. (b) Muzafarov, A. M.; Golly, M.; Möller, M. *Macromolecules* **1995**, *28*, 8444–8446.

(8) (a) Oishi, M.; Minakawa, M.; Imae, I.; Kawakami, Y. *Macromolecules* **2002**, *35*, 4938–4945. (b) Miravet, J. F.; Fréchet, J. M. J. *Macromolecules* **1998**, *31*, 3461–3468. (c) Rubinsztajn, S.; Stein, J. *J. Inorg. Organomet. Polym.* **1995**, *5*, 43–59. (d) Rubinsztajn, S. *J. Inorg. Organomet. Polym.* **1994**, *4*, 61–77. (e) Mathias, L. J.; Carothers, T. W. *J. Am. Chem. Soc.* **1991**, *113*, 4043–4044.

(9) (a) Paulasaari, J. K.; Weber, W. P. *Macromolecules* **2000**, *33*, 2005–2010. (b) Paulasaari, J. K.; Weber, W. P. *Macromol. Chem. Phys.* **2000**, *201*, 1585–1592.

(10) (a) Van Hest, J. C. M.; Delnoye, D. A. P.; Baars, M. W. P. L.; Elissen-Román, C.; van Genderen, M. H. P.; Meijer, E. W. *Chem. Eur. J.* **1996**, *2*, 1616–1626. (b) Gitsov, I.; Frechet, J. M. J. *Macromolecules* **1993**, *26*, 6536–6546. (c) Gitsov, I.; Wooley, K. L.; Hawker, C. J.; Ivaova, P. T.; Frechet, J. M. J. *Macromolecules* **1993**, *26*, 5621–5627. (d) Nguyen, P. M.; Hammond, P. T. *Langmuir* **2006**, *22*, 7825–7832. (e) Santini, C. M. B.; Johnson, M. A.; Boedicker, J. Q.; Hatton, T. A.; Hammond, P. T. *J. Polym. Sci., Part A: Polym. Chem.* **2004**, *42*, 2784–2814.

(11) (a) Marcos, A. G.; Pusel, T. M.; Thomann, R.; Pakula, T.; Okrasa, L.; Geppert, S.; Gronski, W.; Frey, H. *Macromolecules* **2006**, *39*, 971–977. (b) Barriau, E.; Marcos, A. G.; Kautz, H.; Frey, H. *Macromol. Rapid Commun.* **2005**, *26*, 862–867. (c) Wurm, F.; Nieberle, J.; Frey, H. *Macromolecules* **2008**, *41*, 1184–1188.

(12) (a) Shi, G. Y.; Tang, X. Z.; Pan, C. Y. *J. Polym. Sci. Part A: Polym. Sci.* **2008**, *46*, 2390–2401. (b) Wan, W. M.; Pan, C. Y. *Macromolecules* **2008**, *41*, 5085–5088.

(13) (a) B. M. B. Discher, H.; Hammer, D. A.; Discher, D. E.; Won, Y. Y.; Bates, F. S. *J. Phys. Chem. B* **2002**, *106*, 2848–2854. (b) M. H. Maskos, J. R. *Macromol. Rapid Commun.* **2001**, *22*, 271–273. (c) J. C. M. B. Lee, H.; Discher, B. M.; Sheehan, M. A.; Won, Y. Y.; Bates, F. S.; Discher, D. E. *Biotechnol. Bioeng.* **2001**, *73*, 135–145.

(14) (a) Chang, Y.; Kwon, Y. C.; Lee, S. C.; Kim, C. *Macromolecules* **2000**, *33*, 4496–4500. (b) Chang, Y.; Kim, C. J. *Polym. Sci., Part A: Polym. Chem.* **2001**, *39*, 918–926.

(15) Drohmann, C.; Möller, M.; Gorbatsevich, O. B.; Muzafarov, A. M. *J. Polym. Sci., Polym. Chem.* **2000**, *38*, 741–751.

(16) (a) Chen, R. M.; Chien, K.-M.; Wong, K.-T.; Jin, B.-Y.; Luh, T.-Y.; Hou, J.-H.; Fann, W. *J. Am. Chem. Soc.* **1997**, *119*, 11321–11322. (b) Kunai, A.; Toyoda, E.; Nagamoto, I.; Horio, T.; Ishikawa, M. *Organometallics* **1996**, *15*, 75–83. (c) Rickle, G. K. *J. Appl. Polym. Sci.* **1994**, *51*, 605–612. (d) Interrante, L. V.; Rushkin, I.; Shen, Q. *Appl. Organometal. Chem.* **1998**, *12*, 695–705. (e) Grate, J. W.; Kaganove, S. N. *Polymer News* **1999**, *24*, 149–155.

(17) (a) Hölter, D.; Burgath, A.; Frey, H. *Acta Polym.* **1997**, *48*, 30–35. (b) Hanselmann, R.; Hölter, D.; Frey, H. *Macromolecules* **1998**, *31*, 3790–3801.

(18) Bernal, D. P.; Bedrossian, L.; Collins, K.; Fossum, E. *Macromolecules* **2003**, *36*, 333–338.

(19) Pastor-Pérez, L.; Barriau, E.; Berger-Nicoletti, E.; Kilbinger, A. F. M.; Pérez-Prieto, J.; Frey, H.; Stiriba, S.-E. *Macromolecules* **2008**, *41*, 1189–1195.

(20) Dimitrov, Ph.; Rangelov, St.; Dworak, A.; Haraguchi, N.; Hirao, A.; Tsvetanov, Ch. B. *Macromol. Symp.* **2004**, *215*, 127–139, and references therein.

(21) Marciniec, B. In *Comprehensive Handbook on Hydrosilylation*; BPCC Wheatons Ltd.: Exeter, U.K., 1992.

(22) (a) Schlüter, A. D.; Rabe, J. P. *Angew. Chem., Int. Ed.* **2000**, *39*, 864–883. (b) Frey, H. *Angew. Chem., Int. Ed.* **1998**, *37*, 2193–2197.

(23) (a) Hawker, C. J.; Fréchet, J. M. J. *Polymer* **1992**, *33*, 1507–1511. (b) Lach, C.; Hanselmann, H.; Mülhaupt, R.; Frey, H. *Macromol. Rapid Commun.* **1998**, *19*, 461–465. (c) Pusel, T.; Frey, H.; Lee, Y. U.; Jo, W. H. *Polym. Mater. Sci. Eng.* **2001**, *84*, 730–731. (d) Ishizu, K.; Ohta, Y. *J. Mater. Sci.* **2003**, *22*, 647–650.

(24) Lam, D.; Little, S.; Rutherford, J.; Twyman, L. J.; Zheng, X. *Macromolecules* **2008**, *41*, 1584–1586.

(25) Mori, S.; Barth H. G. In *Size Exclusion Chromatography*; Springer-Verlag: Berlin and Heidelberg, Germany, 1999.

(26) Marcos, A. G. *Silicon containing block copolymers. Ph.D. Thesis, University Mainz*, **2006**.

(27) Hölter, D.; Frey, H. *Acta Polym.* **1997**, *48*, 298–309.

(28) Iyer, J.; Fleming, K.; Hammond, P. T. *Macromolecules* **1998**, *31*, 8757–8765.

MA8018427